Petroleum and Coal

Article **Open Access**

Classification and Diagenetic Characteristics of the Permian Sandstones of the Ecca Group in Borehole KWV-1

Sibusiso Maseko, Ronaldo Malapana, Mahlatse M Ntake, Tsibula J Sekantsi, Mokgadi K Teffo and Christopher Baiyegunhi*

Department of Geology and Mining, University of Limpopo, Private Bag X1106, Sovenga 0727, Limpopo Province, South Africa

Received May 23, 2023; Accepted July 20, 2023

Abstract

Several studies suggested that the sandstones of the Main Karoo Basin of South Africa are potential host rock for hydrocarbon exploration in the Main Karoo Basin of South Africa. However, there is still a paucity of knowledge on the effect of diagenesis on the sandstones and diagenesis is one of the most critical processes influencing reservoir rock properties. As a result, this study investigated the effects of diagenesis on the sandstones by subjecting the sandstone to petrographic studies, scanning electron microscope (SEM), energy dispersive x-ray (EDX) and x-ray diffraction analyses. The petrographic studies show that the sandstones of the Ecca Group mainly comprise of feldspar, quartz and lithic fragments, while garnet, hematite and zircon occur in traces. The sandstones have a matrix content greater than 15% but less than 75% and were classified to be graywacke. The SEM and EDX examinations revealed that the diagenetic processes that have significantly affected the sandstones are compaction, cementation, dissolution, replacement and recrystallization. The dominant types of cement in the sandstones are quartz, calcite, and clay cement. Compaction (i.e., concave-convex contact, suture contact) and cementation (i.e., quartz, calcite, and clay) were the main diagenetic processes responsible for the reduction in porosity while dissolution of feldspars and grain fracturing increased porosity. However, the interconnectivity of the pores in the sandstones are low. Porosity is generally well reduced thus making the quality of the reservoir poor.

Keywords: *Diagenesis; Processes; Sandstones; Ecca Group; Karoo Supergroup.*

1. Introduction

The Karoo Supergroup was laid down between 310 and 182 Ma [1-2]. Nearly two-thirds of South Africa is covered by the rocks of this supergroup. The sequence of the Karoo Supergroup is not symmetrical consequently of the orogeny in the south. It has been recorded that, it is much thicker in the south and reaches approximately 12 km, and the sequences are well endowed with fossils [1-2]. Furthermore, it is considered to be thinner in the north as compared to the south, with a maximum surface area of 700,000 km^2. The term "Karoo" was created from the name of the Main Karoo Basin in South Africa to describe the sedimentary rocks common to all basins that developed during the Gondwana period and are similar in age. As a complete record of the late Palaeozoic and early Mesozoic, the Karoo basin is well known and has attracted significant scientific interest [2]. The Karoo Supergroup is mainly a sedimentary basin, although some volcanic rocks are from the Drakensberg Group with minor tuff horizons. The sedimentary rocks making up the Karoo Supergroup are sandstones, claystone, siltstones, mudstone, and carbonate rocks. These rocks have undergone general processes such as lithification and cementation in the transition from loose sediments to consolidated sedimentary rocks, under a process of sedimentary rock formation known as diagenesis.

Diagenesis is a process responsible for changes sediments go through between the period of deposition and metamorphism. Lithification, compaction, cementation, dissolution, mineral replacement, recrystallization, dehydration, and hydration are the processes controlling the physical, mineralogical, and chemical changes undergone by sediments in forming sedimentary rocks. Generally, diagenesis occurs at temperatures less than 250°C and pressures of ~5 kbar [3]. The most important component affecting reservoir characterization is digenesis. As a result, understanding the permeability and porosity of reservoirs, as well as predicting the reservoir characteristics of siliciclastic rocks, requires restoring the diagenetic past. The economic significance of porous siliciclastic rocks as reservoir rocks for petroleum may subsequently be influenced by the strata's diagenetic histories along with their initial depositional features. Petrographic investigations are critical for determining the rate, time, and types by which mechanisms of diagenesis alter the permeability and porosity of sandstones and other clastic sedimentary rocks. To date, in the Ecca Group of the southern Main Karoo Basin, except for the few conducted studies [4-6], there are limited studies that attempt to classify the sandstones and account for the effect of diagenesis on the sandstones.

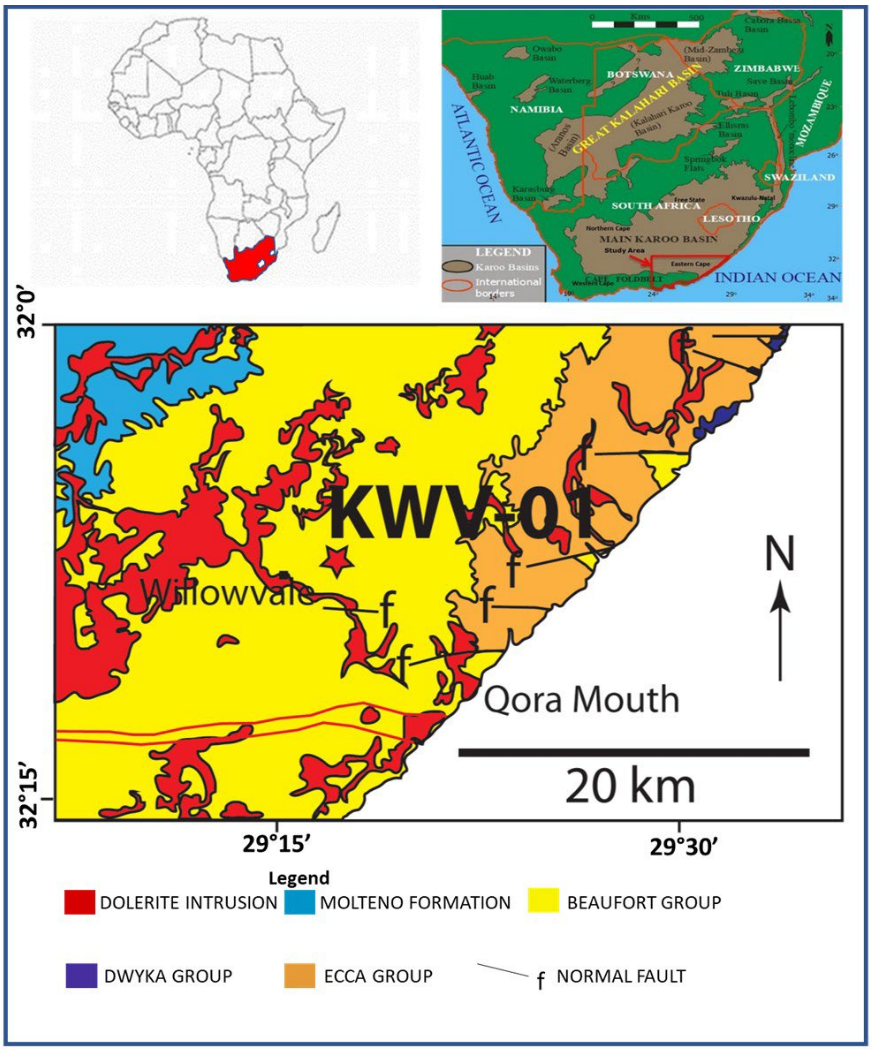

Figure 1. Map showing the study area and the surrounding geology of the area (after [7])

2. Geological setting

The accumulation of the Karoo Basin occurred from the Upper Carboniferous to Middle Jurassic and covers up to 700 000 km^2 of Southern Africa, extending through Lesotho and portions of Eswatini and into Namibia [2,8-9]. Furthermore, the south-eastern Karoo Supergroup has a sediment fill thickness of 12 km. Mafic dyke swarms and basaltic lavas from the Drakensberg Group cover the Karoo succession. The inland sea was connected to the open ocean of the Ecca Group and can be referred to as marine, and the fluvial or continental environment of the Beaufort Group constitutes the Karoo Supergroup stratigraphic succession in the research area [9-10]. [11] determined the lowermost stratum of the Ecca Group lies above the Dwyka Group's glacial succession. Siltstones, mudstones, and sandstones make up the sequence, with minor conglomerates and coal seams forming part of the sequence.

The Bowen (Australia), Beacon (Antarctica), and Paraná (South America) basins are part of the Gondwanan foreland basin, these basins were formed by the converging of plates and tectonostratigraphic terranes formation along Gondwana's southern border boundary [12-16].

The Karoo Basin is a retro-arc, trans-extensional foreland system formed by subsiding and slanting in a strike-slip tectonic regime, with a thin fold belt formed by collisional tectonics and distant southward subduction [9,17-18]. According to [19], the sinking is due to the dynamic topography which can be referred to as the flow of the mantle in conjunction with the sinking blocks. The subsidence was produced by mantle movement, which was complicated by foundation block alterations or variable degrees of foundering, this may have served as the border of a buried basin, affecting the positioning of the continental shelf [17]. The Karoo Basin's sedimentary fill is governed by tectonics and temperature [2,20-22]. Tectonic environments evolved during Karoo times, changing from lithospheric flexure in the south to extensional in the north, following the mechanisms of subsiding, accretion, and orogeny along the paleo-Pacific border known as the Gondwana's Panthalassa boundary.

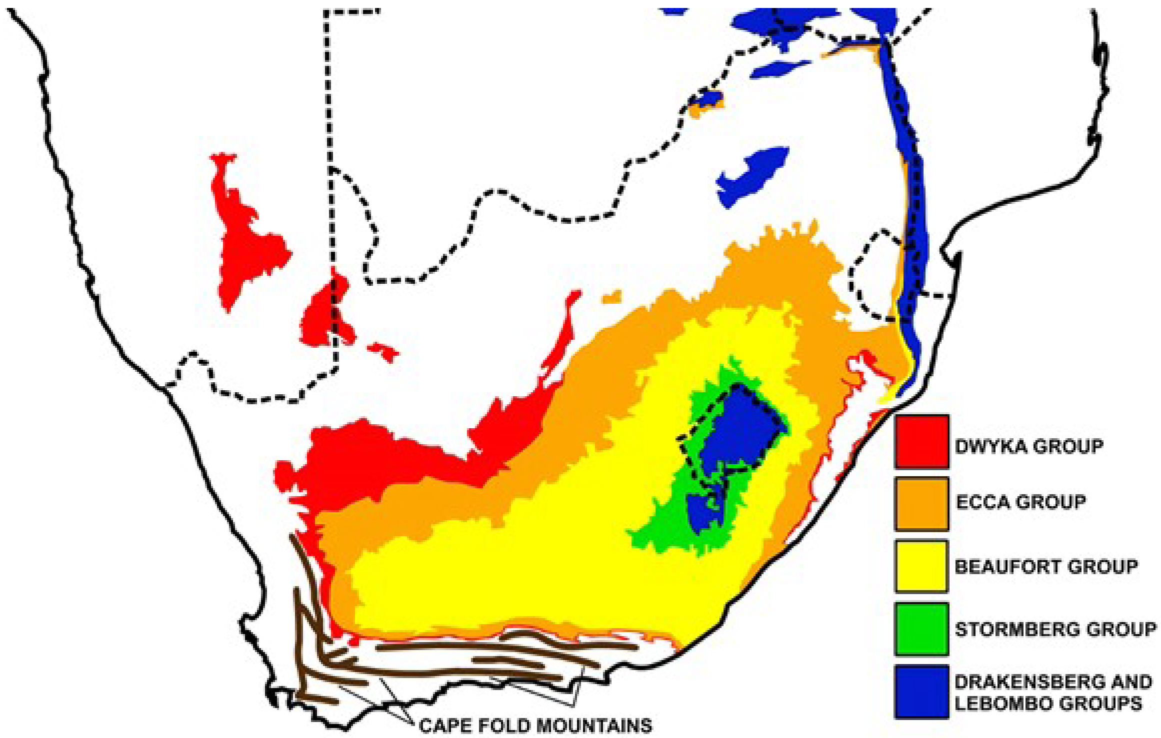

Figure 2. Geological map of the Karoo Supergroup [1]

The Dwyka Group formed between the Upper Carboniferous and the beginning of the Permian period, the Ecca Group is estimated to be Early-Middle Permian, the Beaufort Group is Upper Permian to Mid Triassic, and the Upper Karoo Group is Late Triassic to Early Jurassic, and the Drakensberg Group is dated to be Middle Jurassic, forming Karoo Supergroup sedimentological sequence (Figure 2) [11,23-24]. However, this project is restricted to the Ecca Group. The Ecca Group formed after the Dwyka Group and the before the Beaufort Group, reflecting an Early-Middle Permian age [2]. The Ecca Group in the study region consists of the Collingham, Ripon, and Fort Brown, Prince Albert, Whitehill formations, as well as the Waterford Formation (Figure 3). The Ecca Group is thought to have reached a thickness of 3000 m in the basin's southern half.

Mudstones and clay sedimentation from the Prince Albert Formation took place in the south of the Karoo Basin over the Dwyka Group which is mainly glacial diamictites. The Whitehill Formation, which contains carbon, succeeded it. Shales and sandstones from the Waterford, Collingham, Fort Brown, Ripon and Waterford formations were laid on the underwater deltas, fans, and shelves [25]. Dark carbon-rich shales gave way to siliciclastic sandstones quickly in the Whitehill Formation. In the Whitehill Formation, the transition from dark carbonaceous shales to siliciclastic sandstones was quick, and in the Collingham Formation, turbidite deposits linked to large tuff beds indicate a shift in the tectonic regime [22]. The Ecca Group's proximal turbidite and volcanic ash deposits are observed solely in the Collingham Formation.

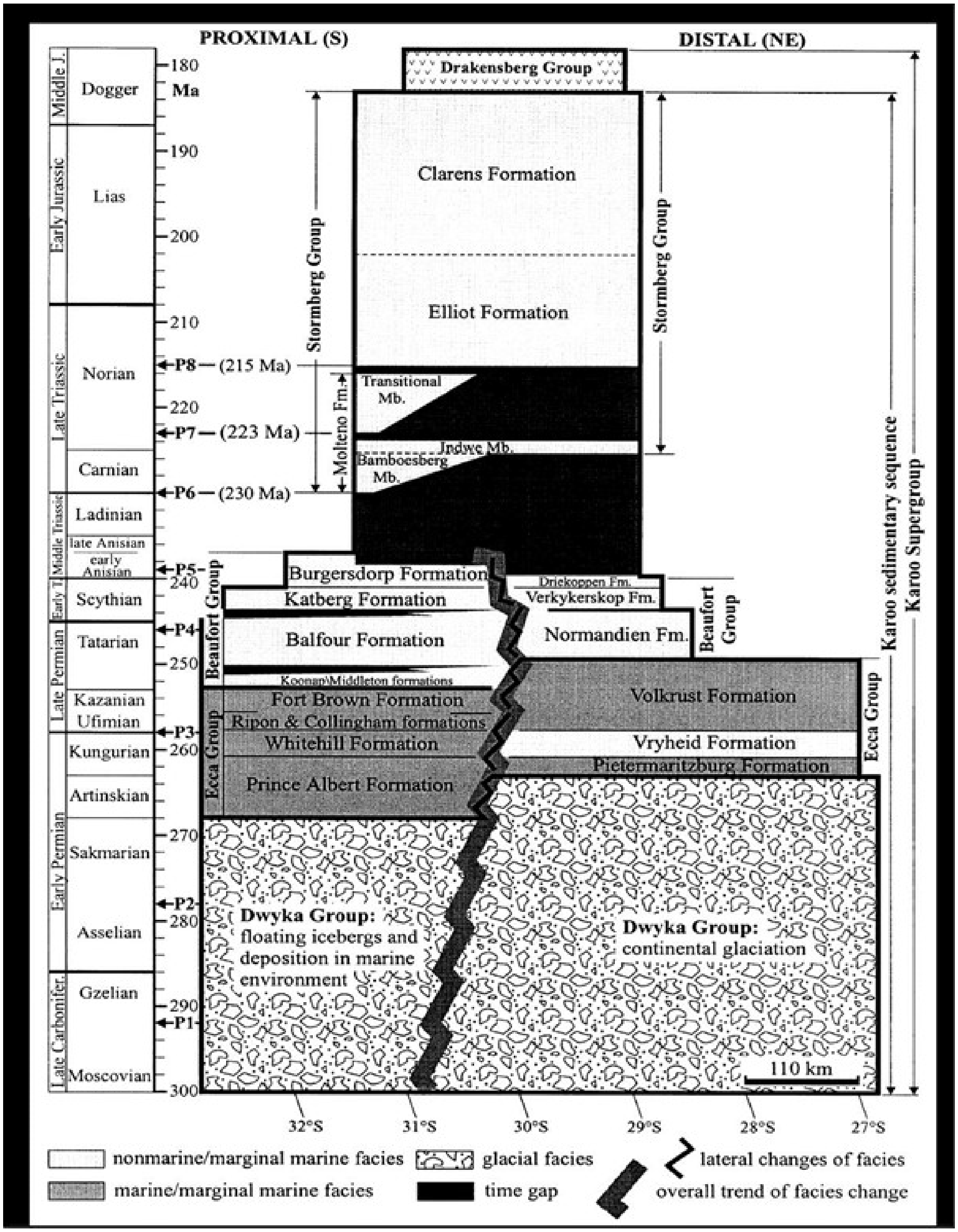

Figure 3. Stratigraphical subdivision of the Karoo Supergroup [26]

3. Materials and methods

Core logging and sampling of borehole KWV-1 was conducted at the Council for Geosciences (CGS) National Core Library in Donkerhoek, South Africa. Thin sections were prepared at the Department of Geology and Mining's thin sections laboratory, University of Limpopo. Petrography studies were carried out through the use of an Olympus polarized light microscope. The modal composition was obtained based on the technique of [27-28] by counting not less than 500 points for each thin section. Framework detrital modes of the sandstones were normalized or recalculated to 100%, and then ternary diagrams of Qt-F-L (total quartz-feldspar-lithic fragments) were plotted to classify the sandstones (Table 1). The collected sandstone samples were crushed using a hammer, samples were broken down into particles measuring around 40 mm, and the separated pieces were sent through a jaw crusher to be crushed, bringing the sizes of the grains to <5 mm. After that, the pulverized samples were fed into the Rig Mill machine for milling to obtain a homogenous texture. To prevent sample contamination, both the riffler and jaw crusher were cleaned after every usage with ethanol, and the finely powdered samples were analysed using X-ray Diffraction (XRD). To completely clean samples and adhere them to a glass microscope slide, Struers specifix resin was mixed with Struers specifix-40 curing agent in a 5:2 weight ratio, the samples were assessed using both secondary electron imaging (SEI) and backscattered electron imaging (BSE) using Energy Dispersive X-ray (EDX), and Scanning Electron Microscope (SEM).

Table 1. Framework parameters of detrital modes

Parameter	Explanation
Q	Quartz (Qm + Qp)
Qp	Polycrystalline quartz
Qm	Monocrystalline quartz
Qt	Total quartzose grains (Qm + Qp)
P	Plagioclase feldspar
K	Potassium feldspar
F	Total feldspar grains (P + K)
Lv	Volcanic-metavolcanic rock fragments
Ls	Sedimentary rock fragments
Lm	Metamorphic lithic fragments
Lsm	Metasedimentary lithic fragments
L	Unstable (Siliciclastic) lithic fragments (Lv + Ls + Lsm)
Lt	Total siliciclastic lithic fragments (L + Qp)
DS	Depth of sampling in meters

Note: n represents the total number of detrital grains (Q-F-L) counted excluding matrix, micas, cement, heavy minerals and carbonates).

4. Results

4.1. Stratigraphy of the Ecca Group in borehole KWV-1

The exploratory well was drilled to a depth of roughly 2353.48 m and there are three groups which have been encountered (Beaufort, Ecca, and Dywka Groups). The following are lithostratigraphic units which were encountered when borehole KWV-1 was drilled, the base up, the geologic sequence of the Ecca Group includes Prince Albert, Whitehill, Collingham, Fort Brown, and Waterford Formations in borehole KWV-1 (Figure 1). It has a thickness of about 2149 m and the sequence has been intruded by multiple dolerites.

The greyish-black shale and carbonaceous shale with sandstone interbeds are found in the Prince Albert Formation and it is 33 m thick. It is generally not well-bedded and has soft-sediment deformation structures with pyrite traces and concretions. Massive black carbonaceous shales with fine-grained sandstone beds with lamination make up the Whitehill Formation which is 26 m thick and lies above the Prince Albert Formation. Furthermore, disseminated pyrite and pyrrhotite with small concentrations can be found in this formation. The Collingham Formation is 243 m thick and overlies the Whitehill Formation, it is composed of thin beds of iron-stained sandstones with greyish-brown shales and a fault zone occurring at a depth of 2185 m while a fracture zone is observed at a depth of 2233 m.

The overlying Ripon Formation is 1116 m thick and has 3 members, Pluto's Vale, Wonderfontein, and the Trumpeters Member. The Pluto's Vale Member has a measured thickness of 695 m and it consists of blackish carbonaceous shale, medium-fine-grained sandstones and siltstone. Fossil twigs, ripple markings, cross-bedding, tuff horizons, and soft sediment deformation structures can be observed in this member. Moreover, a fracture zone and alteration zone can be observed at the depths of 1715 m and 1680 m respectively.

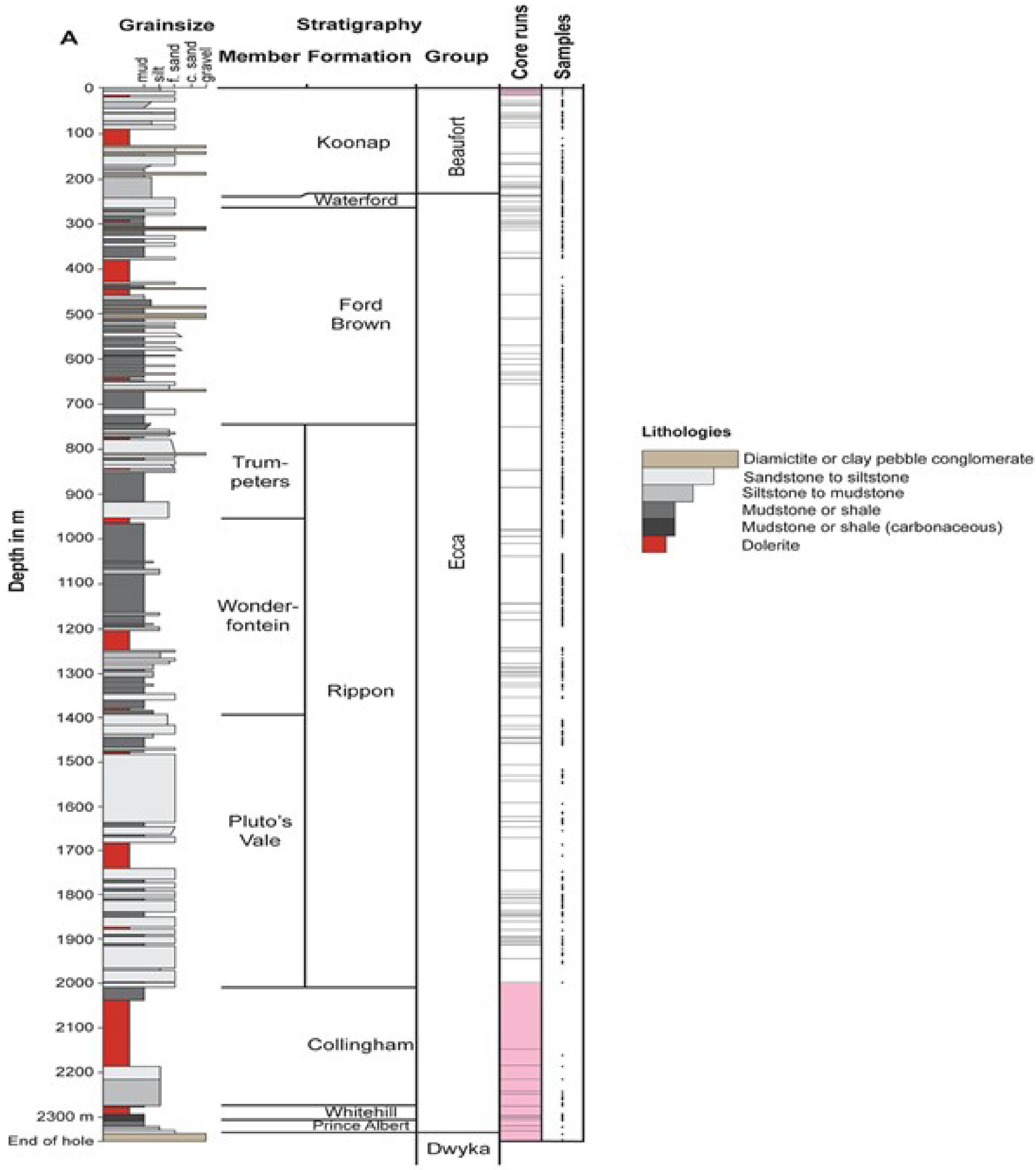

Figure 4. Stratigraphy of borehole KWV1 (modified after [7])

The Wonderfontein Member, which overlies Pluto's Vale Member, has a thickness of approximately 291 m and mainly consists of fine greyish-black shales, fine-grained sandstones, and rhythmic shales with heavy minerals, ripple markings and an alteration zone occurring at a depth of about 1250 m. Above the Wonderfontein Member is the Trumpeters Member with a thickness of 129 m and comprises concentric layers of darkish-grey sandstone and dark grey-to-blackish shale with laminations, soft sediments deformation structures, a fault filled with calcite located at a depth of about 1046 m and it can generally be seen as being well bedded.

The Fort Brown Formation has a thickness of 660 m and it overlies the Trumpeters Member. Generally, it is composed of medium to coarse-grained sandstones, siltstones, conglomerate, breccia, rhythmic shale, carbonaceous shale and ferruginous shales. The Fort Brown Formation is mostly laminated and well-bedded with concretions, soft-sediment deformation structures, ripple markings, and pyrite traces and with two major calcite-filled fracture zone observed at about a depth of 295 m and 306 m respectively.

It is then succeeded by the Waterford Formation, which is mainly mudstones and coarse-grained sandstones. Ripple markings, flaser bedding, concretions and iron-stained layers can be observed in this formation. It is 71 m thick and forms the last layer (formation) of the Ecca Group.

4.2. Petrography

4.2.1. Mineral composition

The framework grains of the studied sandstone samples are presented in Table 2. Quartz ranges from 25.10-34.18% with an average of 30.07%, feldspar ranges from 18.09-37.25% and on average it constitutes about 24.15%, lithic fragments form part of the grain framework and have an amount ranging from 17.33-34.13% with an average of 23.97%, the matrix and cement ranges from 15.74-21.5% with an average 17.43%.

Table 2. Percentage composition of the framework

Formation	DS (m)	n	Qt	F	L	Qm	Qp	Lt= L+Qp	Mx	Acc	Total	Mx (%)	Qt (%)	F (%)	L (%)	Acc (%)	Total (%)
Waterford	199	518	159	131	110	131	28	138	101	17	518	19.50	30.69	25.29	21.24	3.282	100
Waterford	256	507	166	109	125	149	17	142	92	15	507	18.15	32.74	21.50	24.65	2.959	100
Waterford	263	508	147	164	89	123	23	112	89	19	508	17.52	28.94	32.28	17.52	3.74	100
Fort Brown	348	509	174	132	94	148	26	120	93	16	509	18.27	34.18	25.93	18.47	3.14	100
Fort Brown	802	502	126	187	87	112	14	101	79	23	502	15.74	25.10	37.25	17.33	4.58	100
Fort Brown	850	526	139	141	120	129	9	129	113	13	526	21.48	26.43	26.81	22.81	2.47	100
Ripon	925	504	157	104	139	139	19	158	93	11	504	18.45	31.15	20.64	27.58	2.18	100
Ripon	1263	501	130	99	171	94	36	207	85	16	501	16.97	25.95	19.76	34.13	3.19	100
Ripon	1398	521	152	101	147	121	31	178	112	9	521	21.50	29.17	19.39	28.21	1.73	100
Ripon	1534	514	172	93	135	145	27	162	99	15	514	19.26	33.46	18.09	26.26	2.92	100
Collingham	2265	519	166	125	109	158	8	117	109	10	519	21.00	31.98	24.09	21.00	1.93	100
Collingham	2270	515	145	113	142	139	6	148	101	14	515	19.61	28.16	21.94	27.57	2.72	100
Prince Albert	2310	513	153	119	128	133	20	148	101	12	513	19.69	29.82	23.20	24.95	2.34	100
Prince Albert	2322	507	168	111	121	151	17	138	93	14	507	18.34	33.14	21.89	23.87	2.76	100

where DS, n, Qt, F, L, Qm, Qp, Lt, Mx, Acc represents depth of sampling in meters, total number of detrital grains (Q-F-L), total quartzose grains, total feldspar grains, Unstable (Siliciclastic) lithic fragments, monocrystalline quartz, polycrystalline quartz, total siliciclastic lithic fragments, matrix and accessory minerals respectively.

4.2.2 X-ray diffraction

Quartz and feldspar (plagioclase and microcline) were found to have a content ranging from 20-40% and 1-30% respectively. Kaolinite has a range of 4-26%, chlorite ranges from 1-11%, illite from 2-11% and smectite 2-35% (Table 3). The mica minerals have concentrations ranging from 1-18%. Heavy minerals occur as traces (i.e., hematite, garnet, and zircon).

5. Interpretations and discussions

5.1. Mineralogy and classification of sandstones

In the samples from the sandstone of the Ecca Group, quartz is considered to be the most dominant mineral and occurs as both monocrystalline and polycrystalline quartz (Figure 4a and Figure 4b). The quartz mineral consisting of two or more quartz grains is known to be polycrystalline quartz (Qp) whereas, the quartz comprising a single quartz grain are called monocrystalline quartz (Qm). Based on the grain size and shape, the quartz grains are subangular to sub-rounded which is indicative of the travel distance of the grains. Monocrystalline quartz is more common as compared to polycrystalline quartz and quartz cement. Quartz cement can also be observed in these samples as a quartz overgrowth, which is also responsible for holding the grain fragments together (Figure 5b).

Figure 5. Thin section photomicrograph of sandstone showing: (a) monocrystalline quartz (yellow arrows) and polycrystalline quartz (red arrows); (b) depicting quartz overgrowth (blue arrow) and quartz cement (red arrows); (c) Albite; (d) Microcline feldspar; (e) Sandstone lithic (Ls) and Volcanic lithic fragments; (f) Metamorphic and sandstone lithic fragments; (g) Clay matrix and calcite cement; (h) quartz cement

In the sandstones, the feldspars occur as either an alkali or plagioclase feldspar which is microcline and albite respectively. In general, the feldspar grains are subangular to sub-rounded. The amount of feldspar grain is considered the second dominant, after quartz. The feldspar grains are distinguished from each other in terms of twinning, the microcline can be identified by its cross-hatch twinning pattern while the albite is shown by the black-and-white near-parallel striped twinning pattern (Figures 5c and 5d). In the samples, the rock fragments are of sedimentary, igneous, volcanic, and metamorphic origin (Figures 5e and 5f). The cement and fine-grained matrix play part in joining the grains framework together, the matrix is predominantly clay while the cement types are mostly of quartz, clay and calcite (Figure 5g and 5h).

Petrographic studies conducted by [4-5] employing thin sections revealed that the minerals making up the framework of grains of the Ecca Group sandstone are quartz, k-feldspar, mica, and clay minerals such as kaolinite, illite, smectite, and sericite. The aforementioned results are complemented by the findings in this research as they agree. As reported by [6], based on the XRD results, documented that the three formations (i.e., Prince Albert, Whitehill and Collingham formations) have a higher quartz content as compared to other minerals thus, agreeing with the obtained results, although the contents of minerals when contrasted with the result of this research, are higher (e.g., averagely quartz is 48.6%) while the content of quartz has an average of 29.9% in the results of this research (Table 3). This could be because of that only one borehole was considered in this research (KWV-1), while [6] used the average XRD results of 3 boreholes (i.e., KVW-1, SFT2, and SA-1/66) and also their investigations were on the shales, not the sandstones.

Table 3. X-ray Diffraction (XRD) mineralogical composition of the Ecca sandstones

Serial Number	Borehole	Depth (m)	Formation	Plagioclase (%)	Microcline (%)	Quartz (%)	Kaolinite (%)	Chlorite (%)	Mica (%)	Smectite (%)	Illite (%)	Sericite (%)	Hematite (%)	Pyrite (%)	Dolomite (%)	Garnet (%)	Zircon (%)	Zeolite (%)
1	KWV1	525	Fort Brown	30	2	29	6	5	2	20	5	-	tc	-	-	tc	tc	tc
2	KWV1	542	Fort Brown	28	2	30	6	6	2	18	7	-	tc	-	-	tc	tc	tc
3	KWV1	1274	Ripon	20	-	27	6	11	tc	35	tc	-	tc	tc	-	tc	tc	-
4	KWV1	1422	Ripon	19	tc	16	26	9	8	16	5	-	-	-	-	tc	-	-
5	KWV1	1436	Ripon	28	4	40	7	3	5	2	11	-	-	-	-	-	-	-
6	KWV1	1440	Ripon	25	tc	30	6	4	6	28	-	tc	tc	-	-	-	-	-
7	KWV1	1450	Ripon	18	3	34	6	1	9	23	5	-	-	-	-	-	tc	tc
8	KWV1	1465	Ripon	25	tc	32	5	8	2	25	2	tc	tc	tc	-	tc	tc	tc
9	KWV1	1788	Ripon	19	-	28	7	10	1	34	tc	-	tc	tc	-	tc	tc	-
10	KWV1	1893	Ripon	23	3	34	7	6	11	13	tc	2	-	-	-	tc	-	-
11	KWV1	2244	Collingham	11	-	40	12	8	16	12	-	-	-	-	-	tc	tc	-
12	KWV1	2260	Collingham	26	1	31	4	4	1	24	8	-	tc	-	-	tc	tc	tc
13	KWV1	2297	Whitehill	7	tc	30	16	8	15	6	-	tc	tc	7	9	-	-	-
14	KWV1	2302	Whitehill	23	-	37	9	6	14	8	-	tc	-	2	-	-	-	-
15	KWV1	2306	Whitehill	9	-	28	14	4	18	12	-	-	-	9	6	-	-	-
16	KWV1	2314	Prince Albert	15	tc	20	14	8	4	31	-	7	tc	tc	-	tc	tc	-
17	KWV1	2328	Prince Albert	13	tc	23	16	4	6	33	-	3	tc	tc	-	tc	tc	-

Note: sst, mds, sh, tc and - represent sandstone, mudstone, shale, and minerals identified in traces and not detected, respectively

In classifying sandstones, the content of the matrix is a contributing factor to the percentage of the overall framework of grains. There have been many documented proposals on the classification of sandstones, but the sandstones in the study area have been classified using the classification systems by the following researchers [28-31]. According to this prominent classification method postulated by the researchers, rocks which are mostly made up of sand and sediments that are composed of less than 15% matrix are termed arenites, while the ones containing matrix content between 15% and 75% are known to be arkose or wackes, and finally, the rocks containing greater than 75% matrix content are subsequently known to be mudstones or mudrocks (Table 4).

Table 4. Classification of sandstones (after [32])

Serial Number	Bore-hole	Depth (m)	Formation	Plagioclase (%)	Microcline (%)	Quartz (%)	Kaolinite (%)	Chlorite (%)	Mica (%)	Smectite (%)	Illite (%)	Sericite (%)	Hematite (%)	Pyrite (%)	Dolomite (%)	Garnet (%)	Zircon (%)	Zeolite (%)
1	KWV1	525	Fort Brown	30	2	29	6	5	2	20	5	-	tc	-	-	tc	tc	tc
2	KWV1	542	Fort Brown	28	2	30	6	6	2	18	7	-	tc	-	-	tc	tc	tc
3	KWV1	1274	Ripon	20	-	27	6	11	tc	35	tc	-	tc	tc	-	tc	tc	-
4	KWV1	1422	Ripon	19	tc	16	26	9	8	16	5	-	-	-	-	tc	-	-
5	KWV1	1436	Ripon	28	4	40	7	3	5	2	11	-	-	-	-	-	-	-
6	KWV1	1440	Ripon	25	tc	30	6	4	6	28	-	tc	tc	-	-	-	-	-
7	KWV1	1450	Ripon	18	3	34	6	1	9	23	5	-	-	-	-	-	tc	tc
8	KWV1	1465	Ripon	25	tc	32	5	8	2	25	2	tc	tc	tc	-	tc	tc	tc
9	KWV1	1788	Ripon	19	-	28	7	10	1	34	tc	-	tc	tc	-	tc	tc	-
10	KWV1	1893	Ripon	23	3	34	7	6	11	13	tc	2	-	-	-	tc	-	-
11	KWV1	2244	Collingham	11	-	40	12	8	16	12	-	-	-	-	-	tc	tc	-
12	KWV1	2260	Collingham	26	1	31	4	4	1	24	8	-	tc	-	-	tc	tc	tc
13	KWV1	2297	Whitehill	7	tc	30	16	8	15	6	-	tc	tc	7	9	-	-	-
14	KWV1	2302	Whitehill	23	-	37	9	6	14	8	-	tc	-	2	-	-	-	-
15	KWV1	2306	Whitehill	9	-	28	14	4	18	12	-	-	-	9	6	-	-	-
16	KWV1	2314	Prince Albert	15	tc	20	14	8	4	31	-	7	tc	tc	-	tc	tc	-
17	KWV1	2328	Prince Albert	13	tc	23	16	4	6	33	-	3	tc	tc	-	tc	tc	-

where DS, n, Qt, F, L, Qm, Qp, Lt, Mx, Acc represents depth of sampling in meters, total number of detrital grains (Q-F-L), total quartzose grains, total feldspar grains, Unstable (Siliciclastic) lithic fragments, monocrystalline quartz, polycrystalline quartz, total siliciclastic lithic fragments, matrix and accessory minerals respectively.

Using the classification scheme postulated by [31-32], the sandstones can be categorised as wacke or even graywacke because they consist of a matrix content which is greater than 15% but less than 75% (Table 5).

Table 5. Modal composition of the Ecca sandstones

Sample ID	Qt	F	L	Qm	Qp	Lt	Mx	Acc	Total	Mx (%)	QFL	Qt-F-L	Normalized Qt-F-L		
													Qt	F	L
WTF1	159	131	110	131	28	138	101	17	518	19.50	400	400	39.80	32.80	27.50
WTF2	166	109	125	149	17	142	92	15	507	18.15	400	400	41.50	27.30	31.30
WTF3	147	164	89	123	23	112	89	19	508	17.52	400	400	36.80	41.00	22.30
FB1	174	132	94	148	26	120	93	16	509	18.27	400	400	43.50	33.00	23.50
FB2	126	187	87	112	14	101	79	23	502	15.74	400	400	31.50	46.80	21.80
FB3	139	141	120	129	9	129	113	13	526	21.48	400	400	34.80	35.30	30.00
RP3	157	104	139	139	19	158	93	11	504	18.45	400	400	39.30	26.00	34.80
RP4	130	99	171	94	36	207	85	16	501	16.97	400	400	32.50	24.80	42.80
RP5	152	101	147	121	31	178	112	9	521	21.5	400	400	38.00	25.30	36.80
RP5	172	93	135	145	27	162	99	15	514	19.26	400	400	43.00	23.30	33.80
CH3	166	125	109	158	8	117	109	10	519	21.00	400	400	41.50	31.30	27.30
CH4	145	113	142	139	6	148	101	14	515	19.61	400	400	36.30	28.30	35.50
PA3	153	119	128	133	20	148	101	12	513	19.69	400	400	38.30	29.80	32.00
PA4	168	111	121	151	17	138	93	14	507	18.34	400	400	42.00	27.80	30.30

where DS, n, Qt, F, L, Qm, Qp, Lt, Mx, Acc represents depth of sampling in meters, total number of detrital grains (Q-F-L), total quartzose grains, total feldspar grains, Unstable (Siliciclastic) lithic fragments, monocrystalline quartz, polycrystalline quartz, total siliciclastic lithic fragments, matrix and accessory minerals respectively

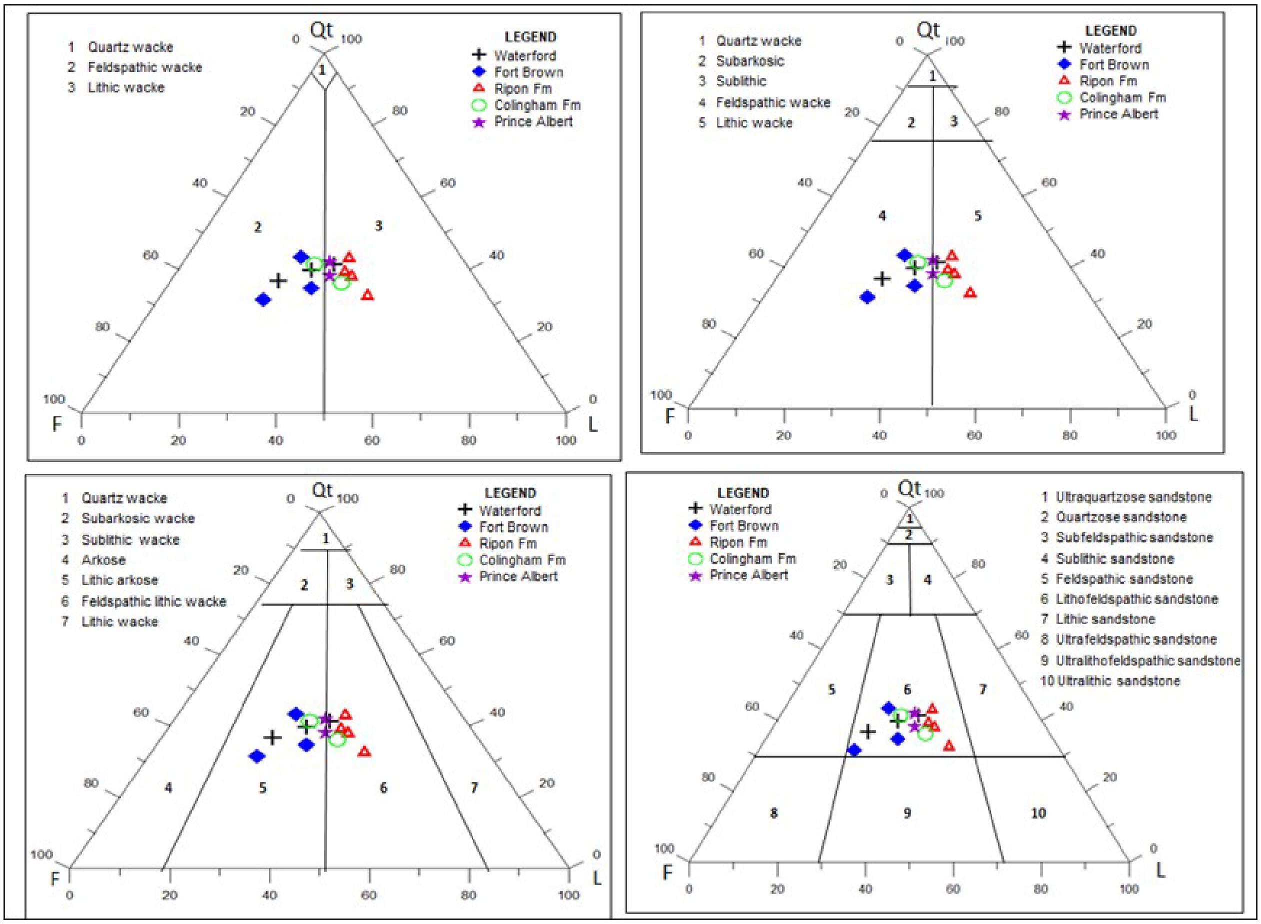

Figure 6. Classification of the Ecca sandstones is depicted in a Qt-F-L ternary plot using the data from Table 5; (a) modified after [31,33]; (b) modified after [29]; (c) modified after [27]; (d) after [27]

Using the classification system postulated by [31,33], the sandstones of the Ecca can be classified as lithic wacke or lithic graywacke (Figure 6), which implies that the framework of grains consists of a rock fragment content of at least 25% with minor amounts of feldspar minerals as compared to the lithic fragments and also quartz minerals [34]. Based on the classification by [27], the sandstones are feldspathic lithic wacke, which means that, in addition to quartz minerals in the framework, the rock is composed of an equal proportion of rock fragments and feldspar minerals. The sandstones of the Ecca Group were classified as being graywacke and were subdivided into three main groups (i.e., lithic graywacke, feldspathic graywackes, and quartz graywackes), and some of the samples were observed to have been moderately well sorted [4,5,35]. The results of this research agree with the findings aforementioned by [4,5,35], as also the sandstones were classified as graywackes with the dominant classes or groups being the feldspathic lithic graywackes and lithic graywacke (Figures 6). [32] suggest that a graywacke has a low silica content compared to other sandstones and instead has more Al_2O_3. This contradicts the findings of this study, which show that graywacke has a high silica content compared to other minerals, ranging from 25.10-34.18% with an average of 30.07%. Given that both authigenic quartz and cement were present as components of the framework grains, the silica (quartz) content may have been higher than expected as a result of overestimation. Furthermore, heavy minerals were only detected as traces. The graywackes in the area of study are the feldspathic lithic graywacke which means in addition to the high matrix content, they have almost an equal proportion of lithic fragments and feldspars, on average the feldspars constitute about 24.15% while the lithic fragments make up an averagely 23.97% of the framework.

[36] suggest that lithic graywacke are matrix-supported sandstones that comprise more fragments of rocks as opposed to feldspar, in addition to quartz which is almost always present along with feldspar and some clay matrix. Moreover, due to the abundance of the matrix in the framework, which could be mostly clay minerals such as illite with some rock inclusions, The sandstone classified as lithic graywacke is considered to have a low sediment maturity and, as a result of the higher matrix content and in the grain framework, it is considered to be poorly sorted, however, the findings of this research do not agree with this as most of the sandstones are moderately well sorted to well sorted.

5.2 Diagenetic processes

5.2.1. Compaction

Compaction occurs as a result of overburdening, as the sediments are exposed to sediment loading which occurs due to continuous burial, therefore increasing the overburden load. It is responsible for the reduction of the volume of the sediments (beds thinning), the expulsion of pore-water contained in the sediments and also decreases the pore spaces [37]. As the volume of sediments is reduced, there is a change in grain packing and contact pattern as the grains become much closer to each other (Figure 7).

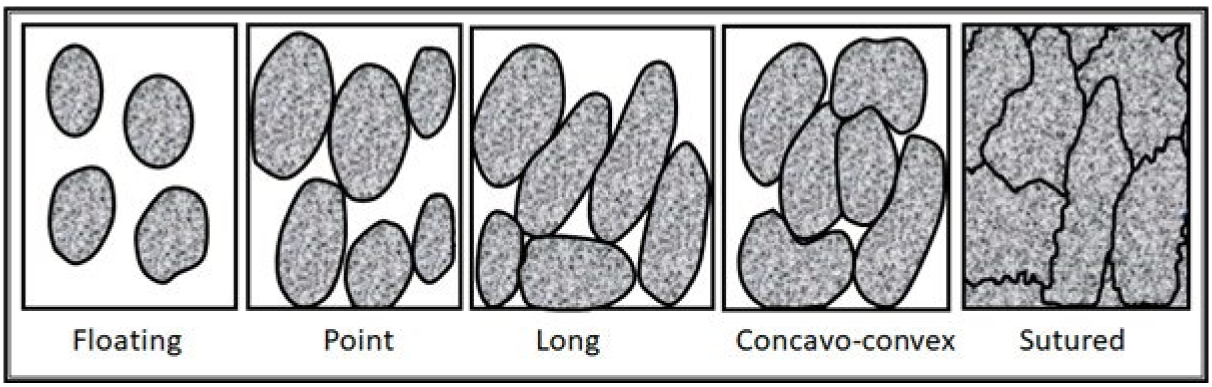

Figure 7. Grain-grain contact patterns variations as burial increases (after [37])

Grain compaction is one of the processes the Ecca sandstones were exposed to, the effects of compaction can be seen in Figures 8a and 8b. The thin section photomicrographs substantiate the occurrence of compaction, as it depicts changes in gran contact patterns and the deformation of minerals such as feldspar and micas through increased pressure due to overburden and also stylolite can be observed (Figure 8a). Throughout the process of continuous burial, Ecca Group sandstones became exposed to medium-high mechanical and chemical compression. It is evident in the transition in grain contacts between adjacent framework grains from floating, long, concavo-convex, and sutured contact patterns (Figures 8a and 8b).

5.2.2 Dissolution

A dissolution crack (Figure 8c) shows that the process of dissolution occurred in the Ecca Group sandstones. The yellow lines show the boundary whereby the minerals were removed, and as there was a void to which other minerals were consequently precipitated into the dissolution crack filling up the space. Organic material exhibiting a blackish colour under the microscopic observations has been precipitated in the void and filled the crack. Dissolution is observed in between grain fragments (i.e., intergranular dissolution) and also occurs inside the grains (i.e., intragranular dissolution). Consequently, as the grain fragments were dissolved, it resulted in the development of secondary pores. The SEM photomicrograph (Figure 8d), shows enhancement of porosity as a result of minerals being removed, the pore spaces are in between grain fragments (intergranular). [35] defined dissolution as a process of partially or completely removing previously present minerals from a solution, leaving void (pore spaces) in the rocks. The material removed or dissolved results in the production of silica which forms and produces quartz overgrowth and cement. Dissolution in the sandstones also occurs at grain contacts and consequently results in the formation of sutured grain contact patterns, if they share the same characteristics such as hardness or solubility (Figure 8a). On the contrary, it results in a concavo-convex grain contact pattern where grains dissolve individually not concomitantly (Figure 8b) [38].

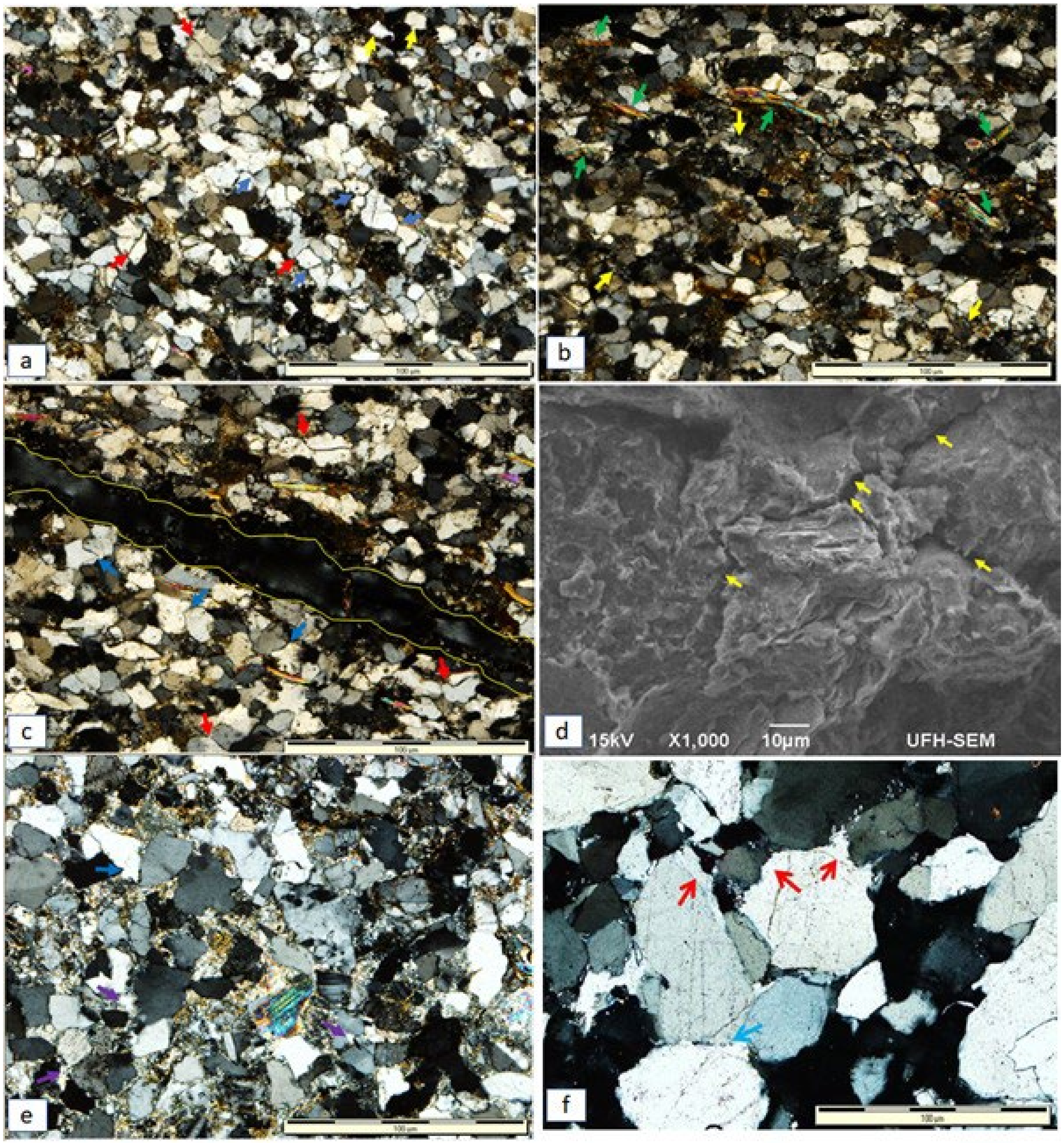

Figure 8. Thin section and SEM (BSE) photomicrographs of sandstone showing: (a) long (red arrows), point (blue arrows) and floating (yellow arrows) contact between grains; (b) feldspar deformation (yellow arrows) and mica deformation (green arrows); (c) dissolution crack (yellow lines), concavo-convex pattern (red arrows) and suture contact pattern (blue arrows); (d) dissolution cracks (yellow arrows); (e) quartz cement (purple arrows) with quartz overgrowth (blue arrows); (f) feldspar cement (blue arrow) and feldspar outgrowth/overgrowth (red arrows)

5.2.3 Cementation

The process of cementation is responsible for binding (i.e., cementing) the grains together as the material becomes precipitated in void spaces of the sandstones, cementation is considered to take place in between grains or within the grains and these are referred to as intergranular or intragranular pore spaces. The processes of cementation can take place at any point of the diagenetic stages (early diagenetic to the uplift diagenetic stage) and various types of grain cementation are observed. The major cement types found on the sandstones are quartz, calcite, and clay cement with minor amounts of feldspar cement.

5.2.3.1 Quartz cementation

In the sandstones, silica material can be seen precipitated in pore spaces forming quartz cement and also syntaxial quartz overgrowth and outgrowth, as another type of silica or quartz cementation (Figure 8e). The quartz cement formed in the early diagenetic history of the sandstones, in a shallow marine environment. The micas and feldspars were subjected to alteration processes, consequent dissolution and alteration and when this occurred it served as a source of the silica that was, in turn, precipitated as quartz cement and also syntaxial quartz overgrowth (Figure 8e). SEM results complement the microscopy analysis because they provide the elemental composition (Figure 9). The high peaks show a high content of silicon and oxygen hence justifying that indeed this cement is quartz cement (SiO_2). Quartz cement is sometimes referred to as silica cement (SiO_2), the silica could have been also originating and derived from pressure dissolution, and dissolution by circulating silica water and is commonly regarded as the main source of silica cementation [38]. When saturation is reached, silica in pore solutions becomes re-precipitated forming quartz overgrowths. Aeolian sandstones may also produce SiO_2 dust when exposed to erosion and this can also serve as a source of silica cement [38]. Furthermore, to fill a pore with cement, the SiO_2-supersaturated fluid must repeatedly pass through the pore.

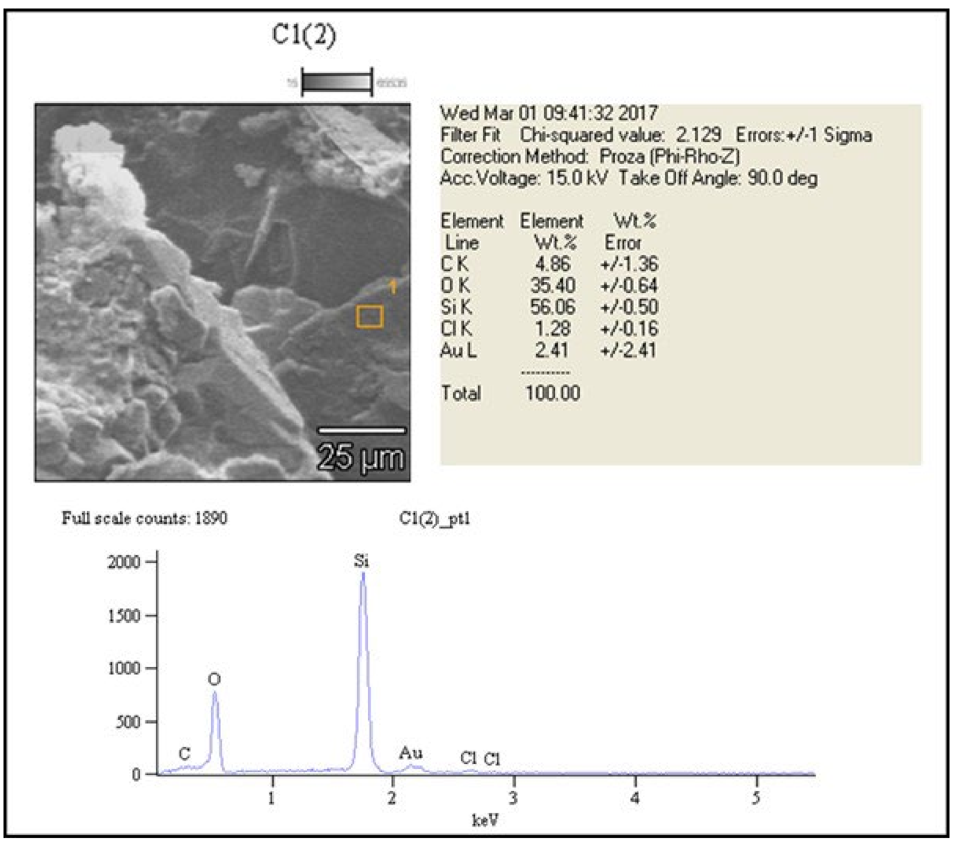

Figure 9. SEM (BSE) photomicrograph showing the occurrence of quartz cement

5.2.3.2 Feldspar cement

Feldspar also forms part of the type of cementation that occurred in the Ecca Group, it is seen precipitated in pore spaces and also occurring as overgrowths around the mineral grains, the feldspar overgrowth can be both polycrystalline and monocrystalline (Figure 8f). The authigenic feldspar cement occurring in the sandstones is albite although microcline is also present as cement. Feldspar cement is the least common kind of cement found in the sandstones of the Ecca Group but has significant value given that these overgrowths, particularly K-feldspar overgrowths, can be radiometrically dated using the K-Ar and $^{40}Ar/^{39}Ar$ procedures [39-40]. Moreover, identifying authigenic feldspars is necessary to comprehend burial-related pore-water compositional changes over time.

The maximum temperature of formation of authigenic feldspars, particularly albite has been documented to have ranged from 105–110°C [41]. Furthermore, the cement might have originated from multiple sources, including the derivation from detrital feldspar grains resulting from consequent dissolution and alteration. Pressure solutions due to sediment loading and burial could also potentially be another source of the feldspar cement.

5.2.3.3 Calcite cement

In addition to the mentioned kinds of cement, calcite cement is found Ecca Group sandstones (Figure 10a). The calcite cement in the sandstones mostly appears as a mineral that fills pore spaces and replaces detrital grains and clay matrix. This may indicate precipitation at various diagenetic stages. Locally, calcite forms in pore voids. It partially or utterly replaces quartz and feldspar grains, typically at their edges. Calcite replaced the detrital feldspar grains and clay matrix after they were altered. The occurrence of the cement is also supported by the SEM photomicrograph (Figure 10b). Researchers including [42-43] proposed that the interaction between an acidic liquid solution comprising carbonate minerals, calcium silicate, or even CO_2 results in the formation of calcite cement, which is a by-product of water-rock contact reaction. Past studies more especially conducted by [44,45], have looked into the organic and inorganic sources of fluid comprising diagenetic carbon dioxide. Additionally, both internal and external sources provided the Ca^{2+} ion necessary for calcite crystallization and precipitation.

5.2.3.4 Clay cementation

Clay cement is one of the frequent types of cement found in sandstones, with kaolinite, smectite, and illite being the most prevalent. Clay cement can be created in various ways, including by altering brittle silicate minerals (i.e., feldspars), and the pseudomorphic or neomorphic change of minerals derived from pre-existing rocks or clay at the start of diagenesis. The recrystallization of the matrix and K-feldspar dissolution resulted in the formation of clay minerals in the sandstones. The cement may have emerged due to the alteration of a clay mineral into another, for example whenever kaolinite/smectite underwent illitization.

5.2.3.4.1 Illite clay

Illite clay fills pores and covers grains, bridging them. The optical properties of the crystals are erroneous since they are often so minuscule. Crystals that protrude perpendicular to the grain and precipitates that coat the grain in small threads are produced by illite (Figure 10c). Illite is typically related to the transformation of kaolinite or smectite as well as the alteration of micas or feldspars, and can also be found as vermicular piled flakes and booklets that look kaolinite (Figure 10c). Illite forms on the surfaces of observed smectite in the form of a curving flake, which produces mixed illite-smectite layers, smectite is seen with a honeycomb-like texture (Figure 10d). The transformation of smectite to illite occurred as the temperature became elevated, and as it further increased it prompted the transition of illite to sericite [44]. Furthermore, the sericite was converted to muscovite by the alteration process. Illite must develop in an environment that contains significant amounts of aluminium (Al), silica (Si), and potassium (K). According to the EDX analysis (Figure 11), the mineral's primary elements are aluminium and silica, with relatively small amounts of K, Fe, and Mg. This is consistent with the illite's chemical formula or composition, which is (K, H_3O) (Al, Mg, Fe)$_2$(Si, Al)$_4O_{10}$[$(OH)_2$, (H_2O)])[4,46]. The formula for illitization is as follows [47]:

$$3Al_2Si_2O_5(OH)_4 + 2K^+ \Rightarrow 2KAl_3Si_3O_{10}(OH)_2 + 3H_2O + 2H^+$$

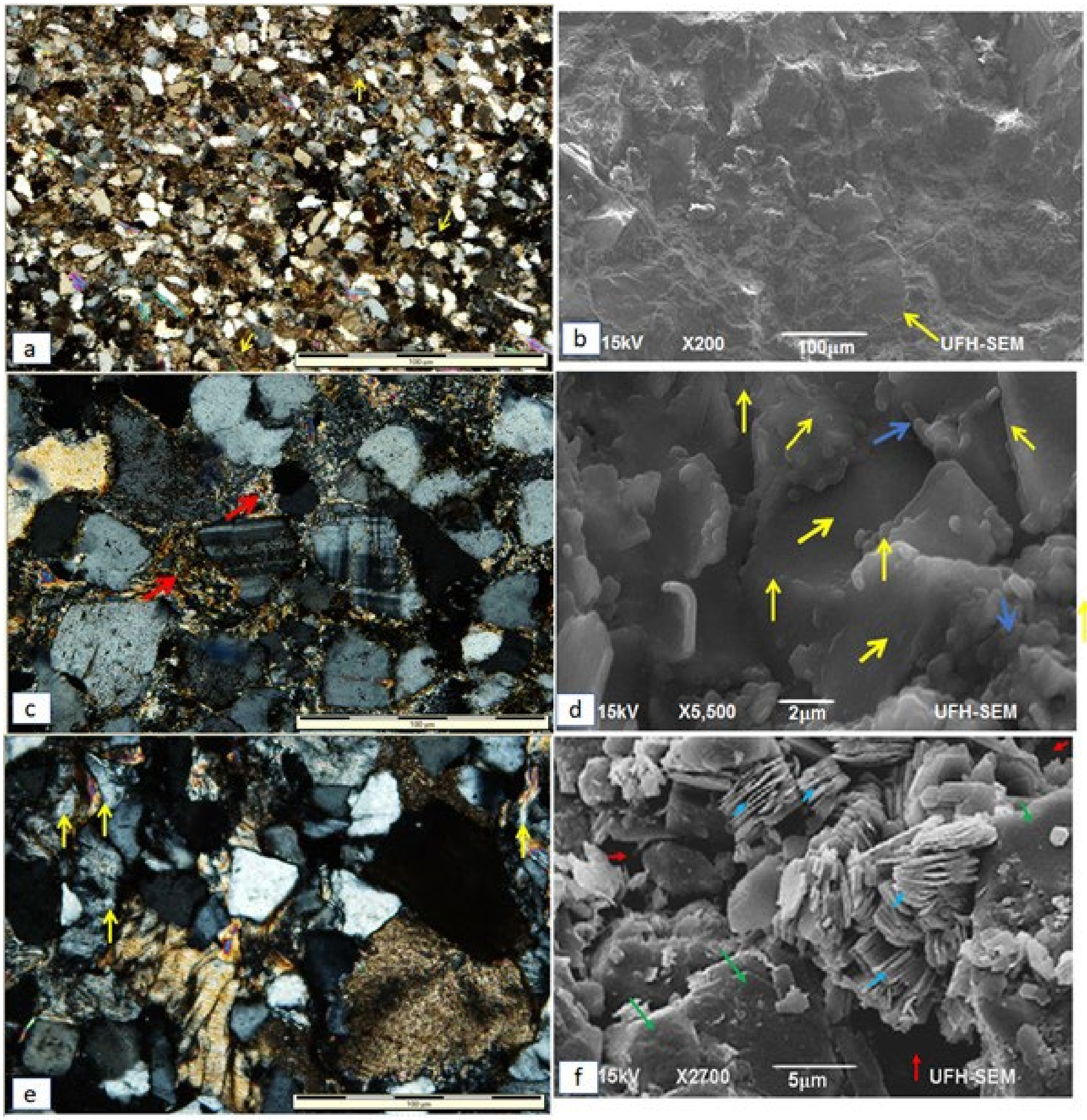

Figure 10. Thin section and SEM (BSE) photomicrographs of sandstone showing: (a) Thin section photomicrograph showing calcite cement (yellow arrows); (b) depicting calcite cement; (c) smectite/kaolinite recrystallization to illite (red arrows); (d) illite growth (blue) on smectite flakes (yellow); (e) alteration of feldspar grains to kaolinite vermicules (yellow arrows); (f) book-page-shaped kaolinite (blue arrows) and SiO_2 cement (green arrows) partly filling the intergranular pores (red arrows)

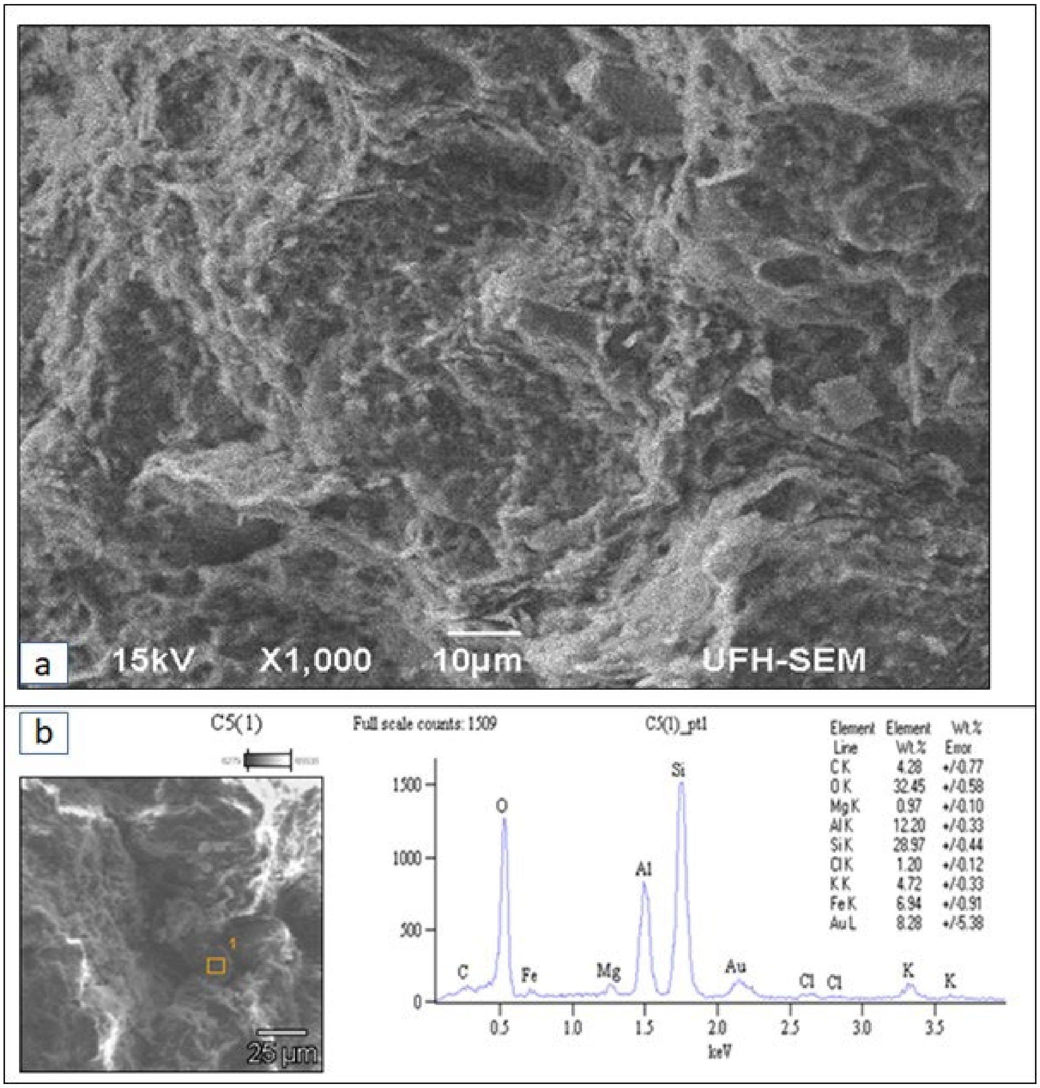

Figure 11. SEM (BSE) photomicrograph illustrating fabric-shaped illite and quartz grains; (b) EDX graph illustrating the composition of illite at a point (orange area)

5.2.3.4.2. Kaolinite clay

Kaolinite is a mineralized aluminosilicate clay that often creates discontinuous pore-refilling cement. Alteration of feldspar is frequently accompanied by kaolinite formation in the sandstones (Figure 10e).

Detrital kaolinite was transported and deposited in the basin, whereas authigenic kaolinite is generated by diagenetic processes. The latter exhibits a perfect crystalline shape under SEM, whereas the past displays erosion and deposition-related characteristics, such as sharp or fractured grain. Clay accordion-shaped flakes exist in the voids occurring in between the grains as crystalline flakes, according to SEM analysis (Figure 10f).

5.2.3.4.3. Smectite clay

In the sandstones smectite clay is found as coatings on grains and according to the SEM analyses, smectite clay appears to have a texture resembling cornflakes (Figures 12a and 12b). According to [48], smectite clays are mostly eogenetic (i.e., early diagenetic stage) cement that forms in an oxidizing environment (i.e., in sodium-potassium-rich pore fluids).

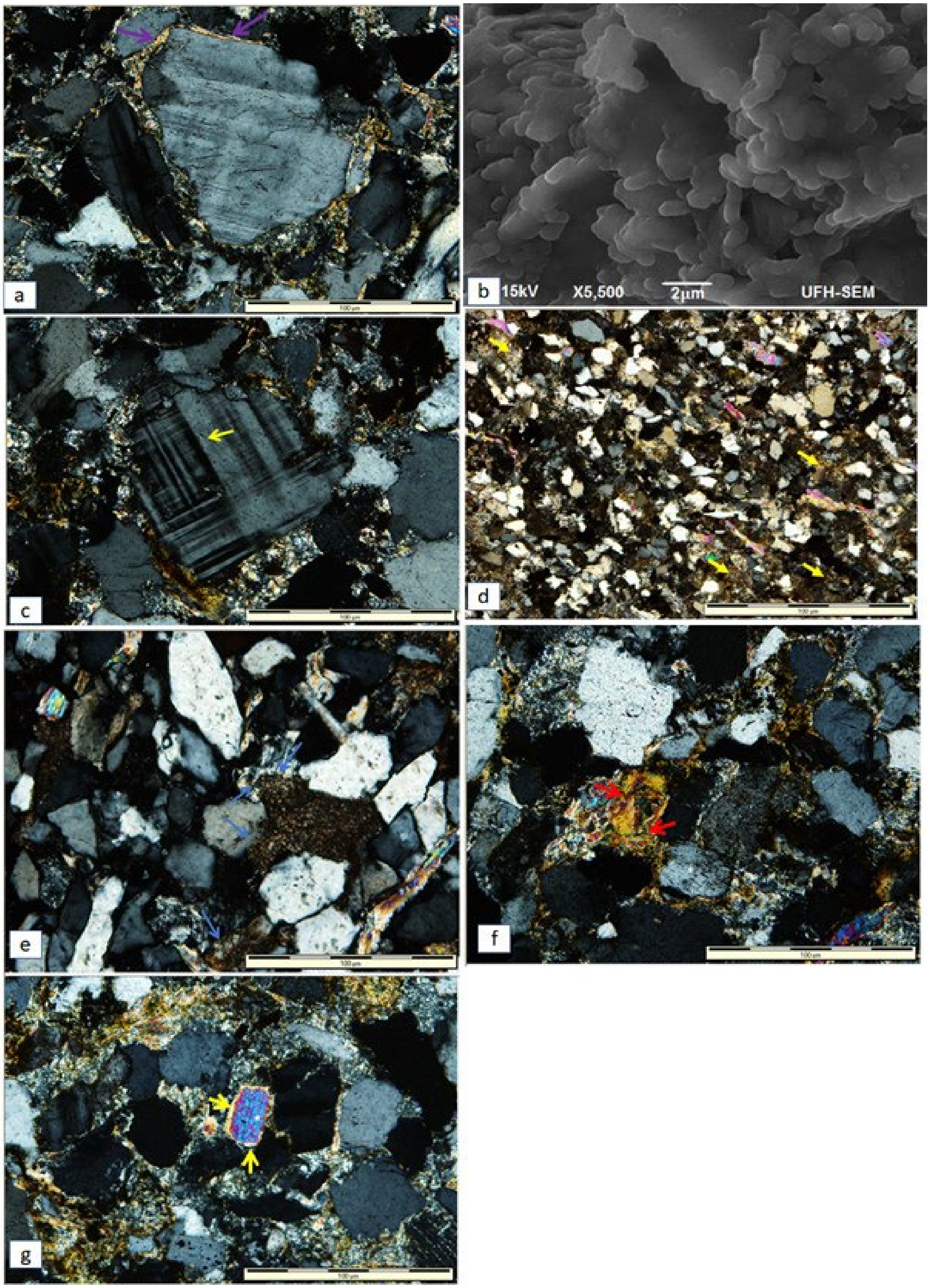

Figure 12. Thin section and SEM (BSE) photomicrographs of sandstone showing: (a) clay matrix (illitization or smectite) around feldspar grain; (b) smectite flakes recrystallized to pelletic and fibrous illite; (c) K-feldspar alteration by albite (yellow arrow); (d) calcite replacement (yellow arrows); (e) clay matrix partially replacing feldspar (blue arrows); (f) recrystallization of clay matrix to sericite (red arrows); (g) change of mica to clay minerals (kaolinite) along its boundary (yellow arrows)

5.2.4. Mineral replacement

When minerals are dissolved, other minerals may be precipitated in their place, in a process known as mineral replacement. The parent or existing minerals may eventually be replaced by the freshly precipitated minerals during this process of dissolution and re-precipitation throughout time. During burial diagenesis, potassium feldspars are prone to change. Mineral replacement is a particularly frequent process within the sandstones of the Ecca Group.

5.2.4.1. Albite replacement

Feldspars are highly prone to alteration if the conditions of their diagenetic environments are changed. The K- or Ca-feldspar framework grains have either been completely or partially substituted by albite, this is substantiated by the sharp edges and corners and smooth crystal faces that characterize the euhedral nature of albite crystals. Albite replaced K-feldspar predominantly in sandstones of the Ecca (Figure 12c).

5.2.4.2. Calcite replacement

In the sandstones, calcite replacement is by far the most dominant, and it is seen replacing both the grain fragments and clay matrix (Figure 12d). The most affected grains were the feldspars because they are least resistant to alteration processes and hence were replaced by calcite. Textural characteristics at the edges of the grains serve as evidence that indeed the calcite is replacing the matrix.

5.2.4.3. Replacement by clay matrix

Potassium feldspar in some instances is replaced by clay matrix (Figure 10e), this is also supported by the textural characteristics displayed at the edges of the feldspar grains. Part of the mineral has been eaten up by the clay minerals, as there is a sharp transition in the feldspar grain to the matrix and also the grains have a jagged-like texture, this displayed that portion of the feldspar grain became unstable and was replaced by the clay minerals.

5.2.5. Recrystallization

Minerals formed at the position they are found in (present position) such as illite, quartz, mica, sericite, feldspars, and chlorite were found to be the altered silica minerals in the sandstones, according to studies made using both SEM and petrography. The clay minerals (i.e., smectite, chlorite, and kaolinite) underwent illitization. Subsequently, illite progressively altered into sericite (Figure 12f) and mica (muscovite) as the temperature rose. The muscovite underwent an additional transformation to become kaolinite, frequently near the edges (Figure 12g). Recrystallization is defined as a change in the shape or size of a mineral or crystals that does not result in a change in the mineralogy or elemental makeup. Microscopic minerals (fine-grained) may grow in size, resulting in coarser-grained textures as pressure and temperature rise due to increased sediment loading and burial depth which increases the geothermal gradient.

5.3. Diagenetic stages

In the sandstones of the Ecca Group, the diagenetic stages are sequentially divided into the early diagenetic stage, the burial diagenetic stage, and the uplift diagenetic stage.

5.3.1. Early diagenetic stage

It takes place in very shallow depths and generally encompasses the change from nonconsolidated sediments to sedimentary rock, it occurs after deposition to shallow burial. There are several factors which affect the early diagenetic stage which include the composition of the sediments, texture, the availability of fluids contributing to the formation of petroleum, and pore water geochemistry. Early diagenetic stages do not show the greatest effect of compaction as compared to the following diagenetic stage (burial diagenesis), in this stage, the floating contact grain pattern is converted to a point and some minor long contact grain pattern (Figure 8a). The formation of some minor cement material also occurred in this stage, such as quartz, clay cement (i.e., smectite, illite and kaolinite) and some heavy mineral coating such as hematite. Pyrite becomes precipitated as the organic material plays a part in diagenetic reactions, where it reacts with oxygen making the environment progressively anoxic and consequently, the hydrogen sulphide reacted with the oxygen to precipitate pyrite. It has been suggested by [46] that the iron might have been sourced mainly from the dissolution of pyroxene, biotite, magnetite and hornblende (Table 5).

5.3.2 Burial diagenetic stage

In Ecca Group sandstones, burial diagenesis occurred after the consolidation of the sediments to hard rock and stopped just before metamorphism [36]. The factors influencing this stage involve elevated values of temperature and pressures and the change in composition of the water contained in the pore spaces. The effects of compaction are much more evident in this stage and induced physical changes such as porosity loss. While processes such as the dissolution of minerals, mineral replacement, and the formation of new cement material constituted to chemical changes the sandstones were exposed to. Progressively the depth of burial increased which changed the pore water chemistry as it encountered the clay matrix, this was then followed by the removal or the dissolution of minerals which were unstable (Table 3).

During the burial diagenetic stage, the following diagenetic processes occurred: chemical and physical compaction, mineral dissolution, recrystallization, precipitation, and mineral replacement (i.e., albitization and sericitization), suture grain contact pattern, deformation, and grain fracturing. As a result of closer packing of grains fragments, compaction contributed to the elimination of pore spaces. With further increases in temperatures and pressures, both feldspar and quartz overgrowth started occurring in the temperature range of 69-80°C, the material might have been sourced from dissolution [44]. Additionally, the transformation of kaolinite to illite or sericite, as well as smectite to illite, sericite, or chlorite, occurred. Albite and illite are produced due to the substitution of potassium feldspars. The partial replacement of other K-feldspars by calcite resulted in the liberation of authigenic quartz as a by-product. Unstable grains released cations into the pore fluids, allowing calcite cement to form in the pore space or replace the matrix and framework grains. The motion of certain $CaCO_3$ ions to the centre in pore-solution within the sandstones is what first caused the creation of calcareous concretions or nodules, which are frequently observed in the sandstones of the Ripon Formation. Moreover, the process of compaction further decreased the volume of sediments causing the thinning of sedimentary beds which also contributed to porosity loss as the grain contact pattern, changed from long, through concavo-convex to suture grain contact pattern (Figures 5a and 5b). As the pore spaces were eliminated in the sandstones, it decreased the interconnectivity of the pore spaces (permeability) and fluid circulation. Stylolite structures formed just before, the fracturing of feldspar and muscovite grains started occurring as a result of increased sediment loading and compaction and there was partial development of secondary porosity as the grains were deformed and bent. The grain fracturing could have been induced by tectonic activity leading to increased grain stress levels [37].

5.3.3 Uplift-related diagenetic stage

Low temperatures and pressures, as well as oxidizing and meteoric pore fluids, are characteristics of the uplift diagenesis stage. Under these new conditions, diagenetic mineral assemblages created during burial diagenesis may be unstable and dissolve or change. Additionally, initial mineral agglomerations might experience further diagenetic changes. Although at a great depth of burial, the Ecca Group sandstones were located in a region where meteoric water was present. It persisted at the surface due to surface weathering and uplift. When the rocks were being uplifted, they were susceptible to acid precipitation. Consequently, the dissolution (de-cementation) of preconceived carbonate cement, enhanced porosity. During the uplift diagenetic stage, kaolinite was formed in response to the feldspar alteration, as the sediments interacted with fresh surface water, which is a contributing process of kaolinite formation (kaolinization) as documented by [49]. It is observed that the change that occurred when the sandstones and mudstones were subjected to the meteoric waters could be linked to the red colouring in the mudstones and shales of the Prince Albert Formation. Illite and pyrite, which are iron-rich minerals, were leached or oxidized, causing the mudstones to become stained or coloured red. Additionally, a source of iron may have contributed to the reddish-brown colouration of the Prince Albert Formation shales, as the removal of hornblende and pyrite occurred due to weathering. The processes which are relatively observed in this stage are the fracturing of grains and dissolution (Table 6).

Table 6. Summarized diagenetic processes and changes in the Ecca Group

	Diagenetic stage	Diagenetic Process	Results
Early diagenesis	Early diagenesis	Organic reworking (bioturbation)	Destruction of primary depositional features Creation of trace fossils (i.e., mottled bedding, burrows, tracks and trails)
		Cementation and replacement authigenesis	Formation of bicarbonate and hydrogen sulphide or pyrite in oxygen-poor environments, and iron oxides in oxygen-rich environments Accumulations of clay cement, quartz and feldspar cement and overgrowths, calcite cement and authigenic clay minerals. Minor lithification due to cementation
Burial diagenesis	Burial diagenesis	Physical compaction	Pore-water expulsion, tighter grain packing, decrease in pore space and bed thinning
		Chemical compaction	Removal of silicate grains, reduction in pore spaces and thinning of bed
		Mineral overgrowth	Quartz and feldspar overgrowth
		Dissolution by pore fluids	Removal in a solution of calcite cement, silicate framework grains, rock fragments, and skeletal materials and by destroying less stable minerals first, additional pore spaces are created (secondary porosity).
		Mineral replacement	Partial to complete replacement of silica minerals by carbonates and clay matrix by new minerals (i.e., replacement of feldspar and quartz by calcite (tend to plug pores and reduce porosity).
		Clay-mineral authigenesis	Alteration of one kind of clay mineral to another (i.e., smectite recrystallized into illite or chlorite, kaolinite recrystallized into illite, illite changed to sericite).
		Compaction and mineral deformation	Concave-convex contact, suture contact, grain fracture and deformation. Destruction of primary porosity
Uplift-related diagenesis	Uplift diagenesis	Dissolution	Partial removal or dissolution of earlier formed carbonate cement (decementation)
		Mineral replacement	Replacement of feldspars, rock fragments and ferromagnesian minerals by clay minerals
		Oxidation	Oxidation of iron-rich volcanic fragments and ferromagnesian minerals (i.e., magnetite, biotite and pyroxenes) to goethite, which later dehydrates with time to hematite. Occasional oxidation of pyrite to hematite, destruction of detrital grains by oxidation

5.4. Diagenetic sequences

A diagenetic pathway and sequence can be created by connecting several diagenetic alterations in the Ecca Group. Table 7 shows the diagenetic pathways and processes that resulted in the formation of various minerals in the rocks of the Ecca Group.

Table 7. Events and the Ecca Group's diagenesis pathway in the research area

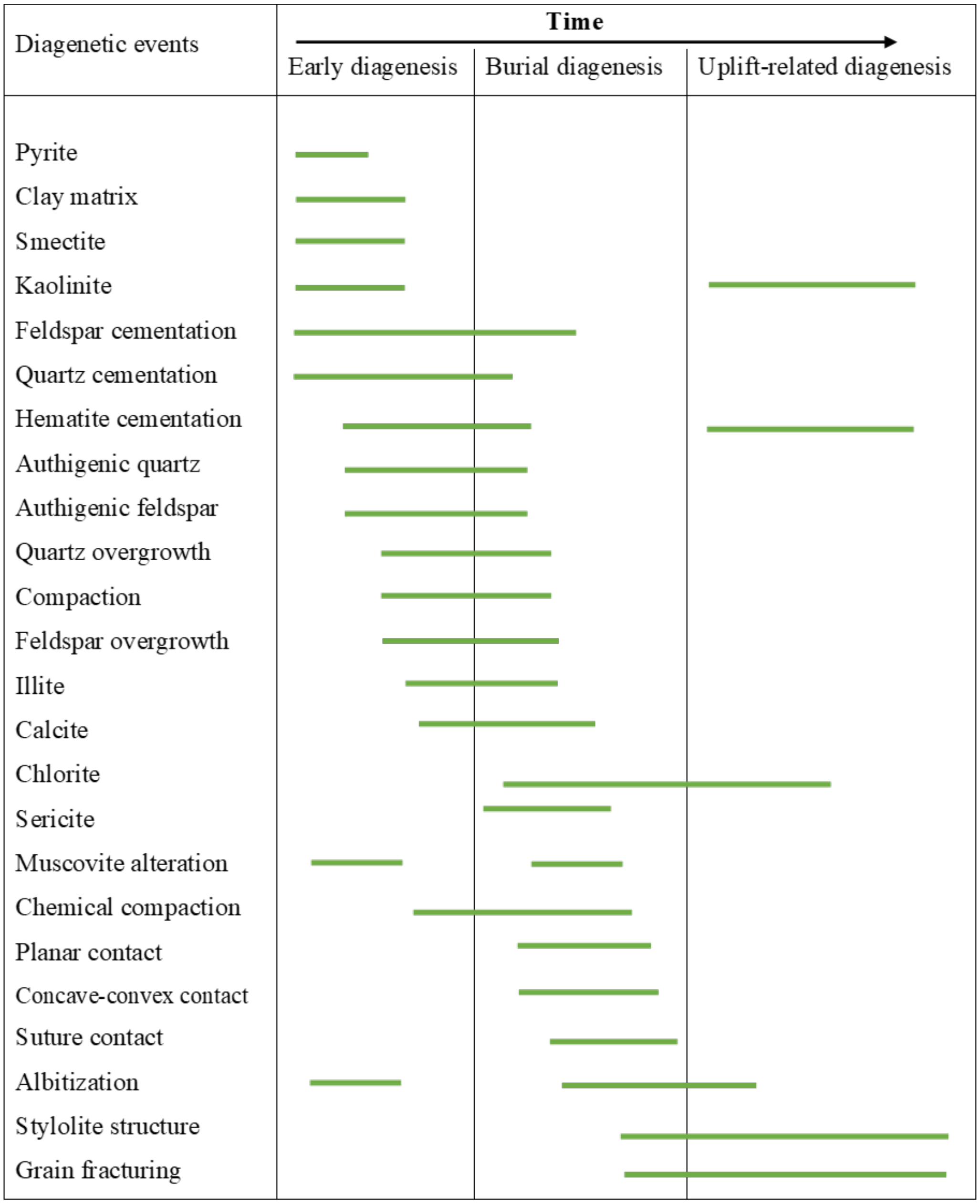

The diagenetic stages can either enhance or decrease porosity [50]. The early diagenetic stage is mostly responsible for the reduction of porosity as the authigenic minerals were precipitated as cementation into pore spaces (i.e., illite, smectite, calcite, silica, and clay cement) and consequently decreasing the permeability of the sandstones (Figure 8-12). In the burial diagenetic stage porosity is negatively affected as mechanical and chemical compaction occurred as shown in Figures 8a and 8b (i.e., pressure solution and sutured grain contact pattern), and also as authigenic quartz and feldspar overgrowth and outgrowth occurred thus affecting the connectivity of the pore spaces (Figure 8e and 8f). On the contrary, the occurrence of the mineral dissolution process (i.e., feldspar and unstable grains) slightly enhanced porosity (Figures 8c and 8d). In the last diagenetic stage (i.e., uplift diagenetic stage), there is both enhancement and reduction of porosity as the feldspar and mica grains were fractured (Figure 8a), and when the kaolinite cement filled the void spaces respectively (Figure 10e and 10f). Diagenesis is responsible for the production of authigenic minerals (pyrite, hematite, calcite). The hydrous silicates, talc/pyrophyllite were detected in the samples of the Ecca Group and could generally be indicative of low-grade metamorphism [51].

6. Conclusions

Petrographic study revealed that the major minerals making up the rocks of the Ecca Group in the study area are quartz occurring as poly- or monocrystalline, feldspars occurring as both albite and microcline and rock fragments with an average of 30.07%, 24.15%, and 23.97% respectively. The matrix and cement were also identified. While XRD results obtained show that quartz range from 20-40% and feldspar range from 1-30%. It was observed that microcline feldspar has lower concentrations and occurs as traces in the Whitehill, Collingham and Prince Albert Formations. Kaolinite ranges from 4-26%, chlorite ranges from 1-11%, illite from 2-11% and smectite 2-35%. In the Whitehill Formation, smectite concentrations are lower than in any other formation in the Ecca Group. Mica ranges from 1-18% while other minerals, particularly the heavy minerals (i.e., hematite, garnet, and zircon) as observed in the XRD results are seen as traces. The sandstones of the Ecca were classified as being graywacke and they are moderately well sorted.

The diagenetic processes and types of cement found in the Ecca Group sandstones were identified using thin sections and SEM+EDX observations. The major processes identified include compaction, cementation, mineral replacement, dissolution, and recrystallization. The identified cement types are quartz, feldspar, clay (i.e., kaolinite, illite, and smectite), and calcite. In the early diagenetic stage, the sediments underwent cementation and light compaction, while greater effects of mechanical compaction, clay mineral cementation, mineral dissolution, pressure solution, and quartz overgrowth were documented in the burial diagenetic stage. Grain fracturing and hematite cement occurred in the uplift diagenetic stage. Compaction led to the reduction of both intra- and intergranular porosity and permeability while dissolution and grain fracturing slightly or insignificantly enhanced porosity but as observed the pores are isolated and thus the permeability is low. The porosity and permeability of the sandstones are well reduced and thus making the reservoir poor as a host rock. The sandstones would require hydraulic fracturing or hydrofracking to release the hydrocarbons.

Acknowledgements

The authors thank the Council for Geoscience of South Africa for allowing access to the core yard.

References

[1] McCarthy T and Rubidge B. The story of Earth and life: a southern African perspective on a 4.6-billion-year journey. Struik, Cape Town, 2005; Chapter 7; p. 192-211.

[2] Catuneanu O, Wopfner H, Eriksson PG, Cairncross B, Rubidge BS, Smith RMH and Hancox PJ. The Karoo basins of south-central Africa. Journal of African Earth Sciences, 2005; 43: 211–253.

[3] Ali Khoudja SA, Chellat S, Hacini M and Semiani A. Petrography and authigenic chlorite in the Siegenian reservoir rocks, Berkine Basin, eastern Algerian Sahara. Arabian Journal of Geosciences, 2020; 13: 1-16.

[4] Baiyegunhi C, Liu K and Gwavava O. Diagenesis and reservoir properties of the Permian Ecca Group sandstones and mudrocks in the Eastern Cape Province, South Africa. Minerals, 2017; 7(6): 60–88.

[5] Baiyegunhi C and Liu K. Sedimentary facies, stratigraphy, and depositional environments of the Ecca Group, Karoo Supergroup in the Eastern Cape Province of South Africa, 2021; 13(1): 748-781.

[6] Geel C, de Wit M, Booth P, Schulz HM and Horsfield B. Palaeo-environment, diagenesis and characteristics of Permian black shales in the lower Karoo Supergroup flanking the Cape Fold Belt near Jansenville, Eastern Cape, South Africa: Implications for the shale gas potential of the Karoo Basin. South African Journal of Geology, 2015; 118(3): 249–274.

[7] de Kock MO, Beukes NJ, van Niekerk HS, Cole D, Robey K, Birch A and Götz AE. Open file progress report on investigation of the southeastern Main Karoo basin borehole KWV-1 NEAR Willowvale in the Eastern Cape Province. Cimera-Karin., December 2015, p. 1-13.

[8] Cole DI. Evolution and development of the Karoo Basin. In: De Wit MJ and Ransome IGD. (Eds.), Inversion Tectonics of the Cape Fold Belt, Karoo and Cretaceous Basins of Southern Africa. A.A. Balkema, Rotterdam., December 1992, p. 87–99.
[9] Flint SA, Hodgson DM, Sprague AR, Brunt RL, Van der Merwe WC, Figueiredo J, Prélat A, Box D, Di Celma C and Kavanagh JP. Depositional architecture and sequence stratigraphy of the Karoo basin floor to shelf edge succession, Laingsburg depocentre, South Africa. Marine and Petroleum Geology, 2011; 28(3): 658-674.
[10] Fildani A, Weislogel A, Drinkwater NJ, McHargue T, Tankard A, Wooden J, Hodgson D and Flint S. U-Pb zircon ages from the southwestern Karoo Basin, South Africa: Implications for the Permian-Triassic boundary. Geology, 2009; 37: 719–722.
[11] Smith RMH. A review of the stratigraphy and sedimentary environments of the Karoo basin of South Africa. Journal of African Earth Sciences, 1990; 10: 117–137.
[12] Veevers JJ, Cole DI and Cowan EJ. Southern Africa: Karoo Basin and Cape Fold Belt. In: Veevers JJ and Powell C. Permian–Triassic Pangean Basins and fold belts along the Panthalassan Margin of Gondwanaland. GSA Memoir, 1994;184: 223–279.
[13] Catuneanu O and Elango HN. Tectonic control on fluvial style: the Balfour Formation of the Karoo Basin, South Africa. Sediment. Geol, 2001; 140: 291–313.
[14] Fouché J, Bate KJ and Van de Merwe R. Regional inversion tectonics along the southern margin of Gondwana. In: De Wit MJ and Ransome IGD. (Eds.), Inversion Tectonics of the Cape Fold Belt, Karoo and Cretaceous Basins of Southern Africa. A.A. Balkema, Rotterdam., December 1992, p. 15–21.
[15] Catuneanu O and Bowker D. Sequence stratigraphy of the Koonap and Middleton fluvial formations in the Karoo foredeep, South Africa. J. Afr. Earth Sci., 2002; 33: 579–595.
[16] Catuneanu O, Hancox PJ and Rubidge BS. Reciprocal flexural behaviour and contrasting stratigraphies: a new basin development model for the Karoo retro-arc foreland system, South Africa. Basin Res., 1998; 10: 41–439.
[17] Tankard A, Welsink H, Aukes P, Newton R and Stettler E. Tectonic evolution of the Cape and Karoo basins of South Africa. Mar. Pet. Geol., 2009; 26 (8): 1379–1412.
[18] Lindeque A, De Wit MJ, Ryberg T, Weber M and Chevallier L. Deep crustal profile across the southern Karoo Basin and Beattie Magnetic Anomaly, South Africa: an integrated interpretation with tectonic implications. South African Journal of Geology., 2011; 114 (4): 265–292.
[19] Pysklywec RN and Mitrovica JX. The role of subduction-induced subsidence in the evolution of the Karoo Basin. Journal of Geology, 1999; 107: 155–164.
[20] Tankard AJ, Jackson MPA, Eriksson KA, Hobday DK, Hunter DR and Minter WEL. Crustal Evolution of Southern Africa, 3.8 Billion Years of Earth History, 1st ed.; Springer-Verlag: New York, 1982; Chapter 11; p. 364.
[21] Johnson MR, Van Vuuren CJ, Hegenberger WF and Key R. and Show, U. Stratigraphy of the Karoo Supergroup in southern Africa: an overview. Journal of African Earth Sciences. 1996; 23(1): 3-15.
[22] Johnson MR, Van Vuuren CJ, Visser JNJ, Cole DI, Wickens HDV, Christie AD and Roberts DL. The Foreland Karoo Basin, South Africa. In Sedimentary basins of the world. Elsevier. 1997; 3: 269-317.
[23] Damiani RJ. Temnospondyls from the Beaufort Group (Karoo Basin) of South Africa and their biostratigraphy. Gondwana Research, 2004; 7(1): 165–173.
[24] Veevers JJ, Cole DI and Cowan EJ. Southern Africa: Karoo Basin and Cape Fold Belt, Permian-Triassic Pangean basins and foldbelts along the Panthalassan margin of Gondwanaland. Geological Society of America, 1994; 184: 223.
[25] Turner BR. Tectonostratigraphical development of the Upper Karooforeland basin: Orogenic unloading versus thermally-induced Gondwana rifting. Journal of African Earth Sciences, 1999; 28(1): 215-238.
[26] Catuneanu O. Retroarc foreland systems-evolution through time. Journal of Earth Sciences. 2004; 38: 225-242.
[27] Dickinson WR, Beard S, Brakenbridge F, Erjavec J, Fergusion R, Inman K, Knepp R, Linberg P and Ryberg, P. Provenance of the North American Phanerozoic sandstones in relation to tectonic setting. Geological Society of America Bulletin, 1983; 4: 222–235.
[28] Dickinson WR and Suczek C. Plate tectonics and sandstone composition. American Association of Petroleum Geologists Bulletin, 1979; 63: 2164–2194.
[29] Folk RL. Petrology of sedimentary rocks, 2nd ed.; Hemphill Publishing Company, Austin: Texas, 1974; p. 182–190.

[30] Dott RH. Wackes, graywacke and matrix: what approach to immature sandstone classification. Journal of Sedimentary Petrology, 1964; 34: 625–632.
[31] Pettijohn FJ, Potter PE and Siever R. Sand and Sandstone, 2nd ed.; Springer-Verlag: New York, 1973; Chapter 11; p. 139.
[32] Pettijohn FJ, Potter PE and Siever R. Sand and Sandstone, 3rd ed., Springer: New York, 1987; p. 553.
[33] Dott RH. Wackes, graywacke and matrix: what approach to immature sandstone classification. Journal of Sedimentary Petrology, 1964; 34: 625–632.
[34] Bjørlykke K. Relationships between depositional environments, burial history and rock properties. Some principal aspects of diagenetic process in sedimentary basins. Sedimentary Geology, 2014; 301: 1-14.
[35] Campbell SA, Mielke P and Götz AE. Geothermal energy from the Main Karoo Basin? New insights from borehole KWV-1 (Eastern Cape, South Africa). Geothermal Energy. 2016; 4(1): 1-19.
[36] Haldar SK and Tišljar J. Introduction to Mineralogy and Petrology.; Elsevier, 2014; Chapter 5; p. 121–212.
[37] Boggs S. Petrology of Sedimentary Rocks, 2nd.; Cambridge University Press, 2009; Chapter 4; p. 111-157.
[38] Tucker ME and Jones SJ. Sedimentary petrology: an introduction to the origin of sedimentary rocks, 4th ed., John Wiley & Sons, 2001; Chapter 1-2; p. 11-103.
[39] Mark DF, Parnell J, Kelley SP, Lee M, Sherlock SC and Carr A. Dating of multistage fluid flow in sandstones: Science, 2005; 309: 2048 –2051.
[40] Hagen E, Kelley SP, Dypvik H and Nilsen O. Direct dating of authigenic K-feldspar, Kjolhamar, sed in: março de 2006 B. Journal of Geological Society, 2001; 158: 801–807.
[41] Schmid S, Worden R.H and Fisher QJ. Diagenesis and reservoir quality of the Sherwood Sandstone (Triassic), Corrib Field, Slyne Basin, west of Ireland: Marine and Petroleum Geology, 2004; 21: 299–315.
[42] Liu Y, Hu W, Cao J, Wang X, Zhu F, Tang Q and Gao W. Fluid–rock interaction and its effects on the Upper Triassic tight sandstones in the Sichuan Basin, China: insights from petrographic and geochemical study of carbonate cements. Sedimentary Geology, 2019; 383: 121–135.
[43] Yuan G, Cao Y, Cluyas J, Li X, Xi K, Wang Y, Jia Z, Sun P and Oxtoby NH. Feldspar dissolution, authigenic clays, and quartz cements in open and closed sandstone geochemical systems during diagenesis: typical examples from two sags in Bohai Bay Basin, East China. American Association of Petroleum Geologists, 2015; 99: 2121–2154.
[44] Morad S. Carbonate cementation in sandstones: distribution patterns and geochemical evolution. In: Morad, S. (Ed.), Carbonate Cementation in Sandstones. International Association of Sedimentologists Special Publication., May 1998, p. 1–26.
[45] Irwin H, Curtis C and Coleman M. Isotopic evidence for source of diagenetic carbonates formed during burial of organic-rich sediments. Nature. 1977; 269: 209–213.
[46] Mosser-Ruck R, Pironon J, Cathelineau M and Trouiller A. Experimental illitization of smectite in a K-rich solution. European Journal of Mineralogy, 2001; 13(5): 829-840.
[47] Jeans CV. The origin of the Triassic clay assemblages of Europe with special reference to the Keuper Marl and Rhaetic of parts of England: Philosophical Transactions of the Royal Society of London, Series A. Mathematical and Physical Sciences, 1978; 289: 549 –636.
[48] Walker TR. Colour of recent sediments in tropical Mexico: a contribution to the origin of red beds. Geological Society of America Bulletin, 1967; 78(7): 917–920.
[49] Bjorlykke K, Elverhoi A and Malm O. Diagenesis in Mesozoic Sandstones from Spitzbergen and the North Sea – a comparison. Geologische Rundschau Journal, 1979; 68: 1152–1171.
[50] Zhang P, Zhang J, Lee Y, Song M, Zhang M, Li J, Ding F and Cheng C. Diagenesis of braided fluvial sandstones and its implications for prediction of reservoir quality: a case study on the Neogene Shawan Formation, Junggar Basin, NW China. Saudi Society for Geosciences, 2013; 8: 29–37.
[51] Oner F and Tas A. Mineralogy and genesis of pyrophyllite deposit on the Poturge Region (Malatya, Eastern Turkey). Geochemistry International, 2011; 51: 143–147.

To whom correspondence should be addressed: Sibusiso Maseko, Department of Geology and Mining, University of Limpopo, Private Bag X1106, Sovenga 0727, Limpopo Province, South Africa;
e-mail: sibusisomaseko129@gmail.com